THE JOURNAL OF Ammonia Energy

Available online at

jae.cardiffuniversitypress.org

ISSN **2752-7735**
The Journal of Ammonia Energy 01 (2023) 118–127

Cardiff University Press | Gwasg Prifysgol Caerdydd

Experimental study on curvature effects and preferential diffusion for perturbed laminar premixed ammonia-air flames

Karan A[a,b*], Dayma G[a,b], Chauveau C[b], Halter F[a,b]

[a] *Université d'Orléans, CNRS-ICARE, 1c avenue de la Recherche Scientifique, F-45071 Orléans cedex, France*
[b]*CNRS-ICARE, 1c avenue de la Recherche Scientifique, F-45071 Orléans cedex, France*

Abstract

Ammonia-air flames are known for low reactivity and have been posing as a huge hindrance in employing the chemical as a sustainable fuel of tomorrow. Curvature is a parameter that could influence the flame structure and so the position of the maximum heat release rate. Flame-acoustic interactions on a Bunsen burner are performed to study the local flame response to highly perturbed flows. NH_2* chemiluminescence is used to study the reactivity of these flames. Non-perturbed flames are used as a reference to understand the inherent behaviour of Bunsen ammonia flames. A case study has been chosen for an equivalence ratio ranging between 1.0 and 1.4 at atmospheric conditions to study perturbed flames. The objective is to study the effect of curvature induced by the perturbations on the reactivity of the flame. It was seen that this given case study was quite complex as the flame response was to multiple factors like the effect of Lewis number, convective-diffusion velocities, decomposition of ammonia into hydrogen, thereby, promoting preferential diffusion of hydrogen in both large-scale and locally for certain cases apart from the generated acoustic perturbation which itself dictates the flow regime of the fresh gases, etc. Since the Damköhler number was around 1, the perturbation time scales and the reactivity time scales were comparable and so none of the effects could be ignored. It was concluded that for richer flames where Le>1, the negative curvature promoted the production of hydrogen leading to local enhancement in reactivity. A change in the local thickness due to the induced curvature was seen for all conditions.

Received: 1st Feb 23; Accepted: 30th June 23; Published: 4th July 23

Keywords: Ammonia hydrogen flames, Laser Diagnostics, Laminar flames, Curvarture

Introduction

Ammonia-air flames are characterized by low flame speeds, thick flames and low reactivity. To make ammonia a viable fuel, its performance must be enhanced and so, the inner structure of the flame must be studied. Upon studying the structure of the flame, different parameters influencing the reactivity can be determined and studied individually. One of the parameters that could influence reactivity is the curvature effect. Turbulent flames are known to induce such curvature and strain which may aid to modify the reactivity of a flame. There are several studies done on swirl flows [1, 2] and turbulent flows [3, 4]. However, turbulence is very complex in nature. The elementary way to study curvature effects is to study a perturbed laminar flame. Most of the literature studies are on blended ammonia fuels [5–9]. There are many ways to study a perturbed laminar flame including flame-vortex interactions and flame-acoustic interactions.

In this work, acoustic perturbations are used to study the curvature effects on premixed ammonia-air flames. There is hardly any experimental work done and literature available on studying perturbed laminar ammonia flames. There are some numerical simulations that have been performed to look into the curvature effects. Netzer et al. [10] studied the curvature effects on NO formation and emphasized the diffusion effects of lighter species and its effect on local curvature for a hydrogen enriched ammonia flame. They demonstrated that for a hydrogen-enriched ammonia flame, there is a change in the rate of preferential diffusion as a function of the orientation of the curvature. From the work done by Wei et al. [11], it can be concluded that the PDF (probability density function) of HRR (heat release rate) indicated that the HRR was more likely to occur at slightly negatively curved flames.

Ammonia is also known to be used as a hydrogen carrier [12–14]. On decomposing 1 mole of ammonia, 3 moles of hydrogen atom can be obtained. Since, it is easier to store and transport

* Corresponding author. E-mail address: alka.karan@cnrs-orleans.fr
https://doi.org/10.18573/jae.16

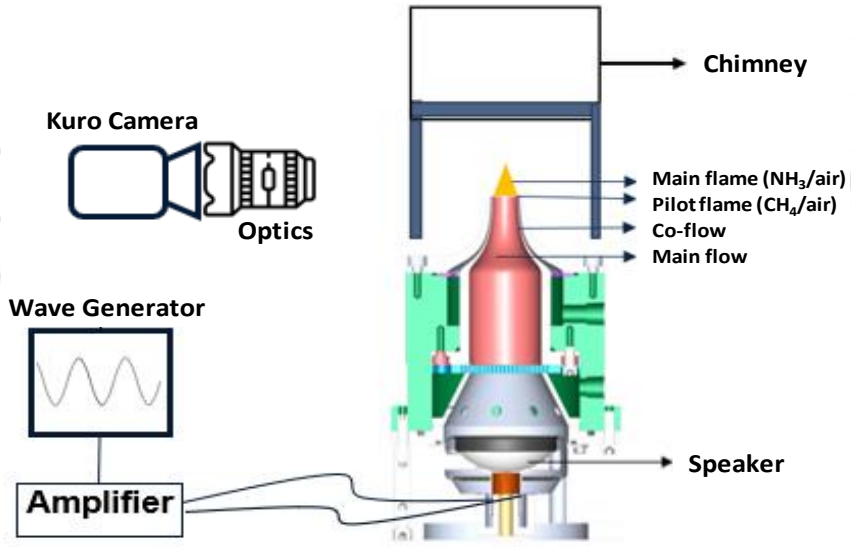

Fig. 1. The schematic diagram of the Bunsen burner with the acoustic system and the chemiluminescence setup

ammonia, it would be an efficient way to use hydrogen stored in ammonia. Rieth et al. [15] simulated lean hydrogen enriched ammonia turbulent flames and have noted that there is a preferential diffusion of light species like H_2 and H especially for highly curved flames. The inner structure of stationary premixed ammonia-air flames on a Bunsen burner at atmospheric conditions for equivalence ratios, φ, ranging between 0.9 and 1.4 was thoroughly investigated. It was concluded that both NH* and NH_2* are good indicators of HRR [16]. Since NH_2* has a higher emission signal when compared to NH*, tracking NH_2* alone as an indicator of HRR should give sufficient information. The primary objective of this study is to focus on the curvature effects induced from the acoustic perturbations on NH_2* or the HRR marker of ammonia-air mixtures for φ=1.0-1.4 at atmospheric conditions on a Bunsen burner. The secondary objective of this study is to see if these high curvature levels promote the decomposition of ammonia to produce hydrogen which can improve the combustion process.

Method

The experiments were performed on a Bunsen burner set-up at atmospheric conditions for φ=1.0-1.4. Figure 1 shows a schematic diagram of the experimental setup. A pilot flame consisting of methane-air at stoichiometry is used to stabilize the main flame. Tests have been carried out to ensure that there is no interference of the pilot flame with the parameters of interest that are monitored in this study. Moreover, the main study has been formed away from the base of the flame. Rotameters are used to control the flow of the pilot flame and mass flow controllers are used to control the feed to the main flame. The mean velocity of the fresh gases at the exit of the burner ranged from 0.18 to 0.20 ms^{-1}. The burner diameter at the exit is 15 mm. A chimney was added to the burner to reduce the flame flickering which resulted from the air entrainment. For an acoustic generation, a speaker is placed at the bottom of the burner. The speaker that was used is an Aura NSW 3-193-8A. The range of frequency of the speaker is 50-100 Hz and its operating power is at 20 W. This speaker was connected to an amplifier which amplifies the signal coming from a wave generator. The amplitude and the frequency can both be controlled with this wave generator. The type of wave needed to be generated can also be monitored here. For this study, only sinusoidal waves that start from 0 V to the desired amplitude were used. A low-speed camera with high resolution (Back-illuminated sCMOS Kuro with a frame size of 2048 × 2048 pix^2) was used to capture the images and the exposure time was set to 1 ms. An objective lens used for the visible range spectrum is attached to the camera. For the non-perturbed case, the experimental set-up was the same except the speaker was not used.

Table 1. Properties of the test cases

φ	D($10^{-5}m^2s^{-1}$)	k (10^{-3} W $m^{-1}K^{-1}$)	Le
0.9	2.102	27.39	0.93
1.0	2.103	27.48	1.00
1.1	2.106	27.56	1.10
1.2	2.109	27.64	1.10
1.3	2.112	27.71	1.09
1.4	2.115	27.86	1.06

The exposure time for this case was extended to 200 ms to have a better image quality. The experimental conditions were slightly extended towards the leaner side of the experimented limits i.e. for an equivalence ratio ranging between 0.9 and 1.4. Studying perturbed flames at φ=0.9 was not easy due to the low signal to noise ratio and due to non-periodic local extinctions for the given perturbation conditions. To monitor NH_2*, an Edmund optics filter with a diameter of 50 mm centred at 632 nm with a bandpass width of 10 nm was used. For the perturbed flame case, it was seen that upon mounting the filter onto the objective lens, the signal-to-noise ratio for this dynamic flame was too low. Since there are several bands of NH_2* emission peaks in the visible region, tests were done to study and compare the images of stationary flames with and without the NH_2* filter and it was concluded that indeed, without using the NH_2* filter collective information on all NH_2* band spectrum is obtained. The conversion factor is 1.67 x 10^{-2} mm/pix for those cases with the NH_2* filter (perturbed case) and 1.75 x 10^{-2} mm/pix for those cases without the NH_2* filter (non-perturbed case). Figure 2 represents the comparison of a non-perturbed flame with and without the NH_2* filter. It can be seen that the two flame images are identical except for the fact that the case with no filter has higher signal when compared to the case with the filter.

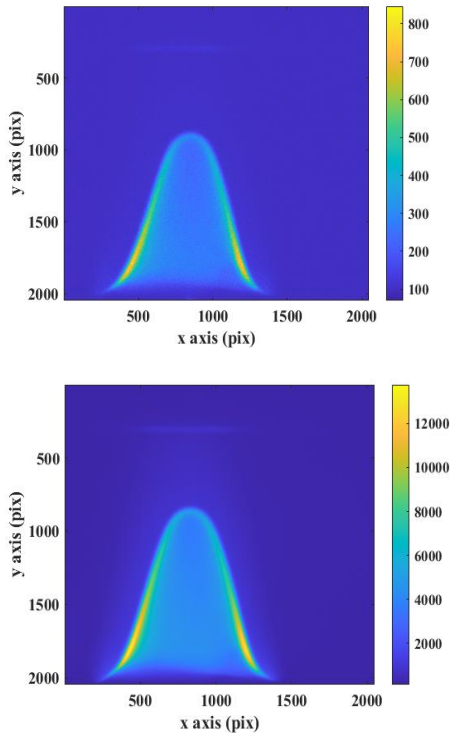

Fig. 2. Top) Raw image of the flame using NH_2 * filter with the visible range objective lens; Bottom) Raw image of the flame without the NH_2 * filter with the visible range objective lens.

To set the test conditions, the response of the flame to both the forcing amplitude and the forcing frequency as well as the interaction between the flow of the fresh gases and the acoustic perturbation must be understood. As the forcing amplitude increases keeping all other conditions constant, the flame tends to elongate subsequently leading to the formation of pockets of fresh gases. As the forcing frequency increases, the flapping behaviour of the flame increases for up to a certain value of frequency beyond which any increase of the forcing frequency does not see any impact on the flame response. This value of frequency depends on the initial flow conditions. On varying the equivalence ratio, it was seen that the weak flames are strongly affected by the perturbation. The magnitude of the curvature of the flame front for the same perturbation conditions was highest for the leanest flame. Indeed, the flow is controlled by both outlet velocity of the fresh gases and acoustic perturbations, and the flame response also depends on the equivalence ratio. According to Birbaud et al. [17] a critical Strouhal number, St_c can be used to divide the flow into three regimes:

- For St < St_c, the flow is convective in nature,
- For St = St_c, the flow is of mixed type,
- For St > St_c, the flow is dominated by acoustics.

St_c is flame geometry dependent and is expressed as S_L/ U_o where S_L is the laminar flame speed and U_o is the convective flow velocity which can be measured using systems such as PIV (particle image velocimetry). Strouhal number, St is defined as:

$$St = \frac{fD}{U_o} \quad (1)$$

where f is the forcing frequency, D is the diameter of the burner exit, and U_o is the convective flow velocity. On understanding the flame response to forcing amplitude and frequency and on identifying the required flow regime i.e. an acoustic-dominated flow, the test conditions have been set with a forcing amplitude of 0.5 V and a forcing frequency of 40 Hz. The setting of this voltage for changing the amplitude depends on the acoustic system. Since, the objective of this work is to study the curvature and preferential diffusion effects, the velocity or the pressure fluctuation at the exit of the burner caused by this setting is not measured.

Results and Discussions

Table 1 details the properties of the gas mixture [18, 19]. D and k represent the mixture diffusivity and thermal conductivity respectively calculated based on the mixture. The non-perturbed cases are first studied to understand the distribution of the HRR marker - NH_2* all along the flame. Figure 3 represents the inverse Abel transformed images of

the chemiluminescence of NH_2* for φ=0.9-1.4 with a normalized colour bar. Each image has been normalized against the maximum intensity in the image. The Lewis number, Le, increases with equivalence ratio and is close to unity [18]. It can be seen that the NH_2* distribution all along the flame is not homogeneous and is different for each equivalence ratio.

By convention, negative curvature is defined for a concave flame in the direction of the burnt gas and a positive curvature is defined for a convex flame in the direction of the burnt gas. For the leanest case, the base of the flame has a positive curvature which then tends to zero and then towards negative at the tip of the flame. Near the base of the flame, there is a local change of kinematic equilibrium and so, the local flame speed is higher than the unstretched laminar flame speed. The reactivity at the base and the sides of the flame is significantly higher and is diminished when encountering a negative curvature at the tip of the flame. Lesser reactivity at the tip of the flame is expected when Le<1. As the equivalence ratio increases there is no more positive curvature at the base of the flame. The reason for the enhanced intensity on the sides closer to the base of the flame is probably attributed to diffusion-convective velocities. Here, the convective velocity is about 25 times more than the diffusion velocity of ammonia into the air at the exit of the burner. The diffusion velocity of ammonia into the air was calculated using Fick's law. It is understood that ammonia decomposes into lighter species whose diffusion velocity is much higher than the convective velocity. The preferential diffusion of H_2 and other species towards the sides plays a major role in enhancing the local reactivity. For this reason, the intensity or reactivity is higher towards the sides of the flame closer to the base compared to the tip of the flame. The effect of preferential diffusion on the reactivity of curved flames has been highlighted by Mizomoto et al. [20]. On simulating a 1D freely propagating flame using Chemkin-Pro, it was seen that indeed there was a decomposition of ammonia to hydrogen via $NH_3 + H = NH_2 + H_2$ even at a lower temperature. The kinetic scheme that was chosen for simulations is the reaction mechanism proposed by Stagni et al. [21]. This mechanism was chosen as a result of performing a brief literature review on the existing mechanisms for ammonia combustion. The premixed laminar flame speed calculator in Chemkin-Pro was used. The curv and grad were set to 0.01 and the length of the domain was set to 2 cm. The decomposition reaction was identified by performing a reaction pathway analysis at regular distances/temperatures in the domain. By looking into the mole fraction of H_2 produced for each equivalence ratio, it was seen that the richer the flame, the more is the amount of H_2 produced. The effect of the preferential diffusion of lighter species like H_2 towards the side of the flames still exists but becomes less significant with the increase in the equivalence ratio. For the cases φ=1.2-1.4, where the Le is slightly more than 1, a local enhancement of reactivity is seen at the tip of the flame (negative curvature) but this relative increase of intensity is not distinctly seen like the case of leaner/near stoichiometric cases where the decrease (in this case as Le≤ 1) in the local intensity is noticeable. This is because the amount of H_2 produced is higher and so there is still some preferential diffusion towards the sides of the flames. From the work done by Chen et al. [22] it has been reported that for richer flames the HRR is more at the tip of the flame and the production of H_2 is enhanced at this curvature. It may be said that for lean and near stoichiometric premixed ammonia-air flames, the large-scale preferential diffusion effects are more apparent than richer flames.

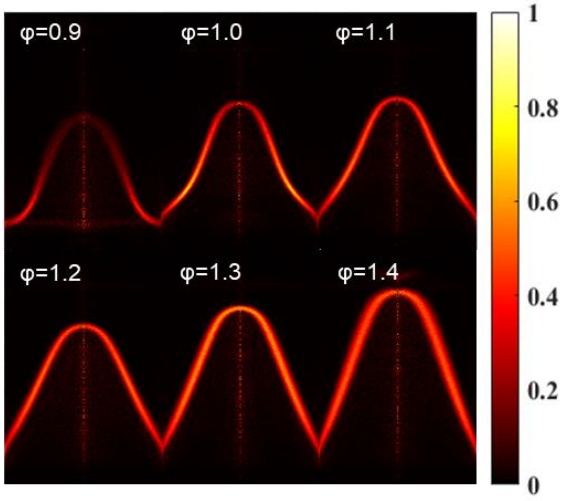

Fig. 3. Chemiluminescence of NH_2 * for non-perturbed flame with normalized intensities showing the diminished effects of large-scale preferential diffusion towards the sides of the flame as a function of equivalence ratio.

Perturbed flames are studied to understand the effect of the curvature on the reactivity of the flame. To study the curvature effect for the given test condition, it was ensured that a similar flame response mode was captured i.e. a similar flame shape was captured for different equivalence ratios. This was done to ensure that uniform parameters are maintained for all conditions. As shown by [23–25], the total stretch K can be decomposed into a tangential strain and a flame propagative/curved character K_c, where K_c is mathematically defined as twice the product of flame displacement speed and mean curvature. As discussed in [16], the strain rate component is quite low due to the low flow velocities and so, only the curvature is focussed.

To study curvature, initially, the mean curvature was obtained to quantify the curvature effect. However, it was seen that the flame response was too complex and so, the two principal curvatures k_1 and k_2 were used. k_1 is defined as the principal curvature along the plane and k_2 is the curvature in the circumferential direction. The mean curvature is simply the average of these two principal curvatures. When the flame is represented in cylindrical coordinate systems with h in the span-wise direction and r in the radial direction, k_1 and k_2 can be mathematically defined as [26]:

$$k_1 = \dot{r}\ddot{h} - \ddot{r}\dot{h} \quad (2)$$

$$k_2 = \frac{\dot{h}}{r} \quad (3)$$

where the dot signifies with respect to the curvilinear coordinate s which is expressed as:

$$\int_0^{\tau} \sqrt{\left[\frac{\partial r}{\partial \varepsilon}\right]^2 - \left[\frac{\partial h}{\partial \varepsilon}\right]^2}\, \partial\varepsilon \quad (4)$$

With ε being a virtual curvilinear abscissa along the meridian curve with a constant interval, $\partial\varepsilon$ equal to one.

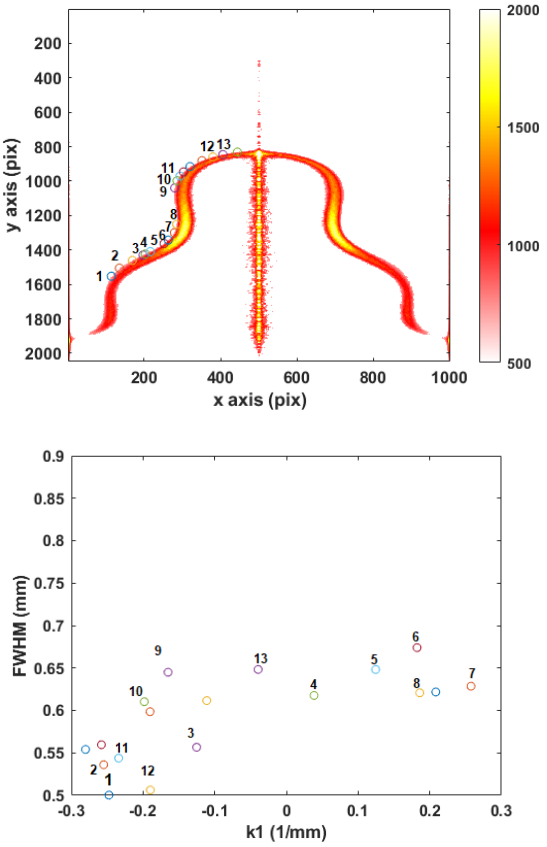

Fig. 4. Top) Inverted Abel transformed image of the flame response for φ=1.0 with the points of interest depicted in coloured loops and numbers; Bottom) thickness vs k1 for the corresponding points.

Four different parameters: k_1, k_2, thickness along the normal to the front, and maximum intensity along the normal to the front were all plotted against the flame contours. Thickness is defined as the FWHM (full width at half maximum) along the normal of the contour when the signal is fitted against a Gaussian plot. To understand the complete response of reactivity, the integrated intensity along the normal must be monitored. Once again, plotting curvature against integrated intensity was too complex and so this parameter was further divided into two basic parameters: thickness and maximum intensity along the normal to the contour. After careful examination, it was seen that the effect of k_1 and thickness along the contour seemed to be correlated but when it came to understanding the maximum intensity and k_2, it was seen that their effect for all equivalence ratios was not very apparent.

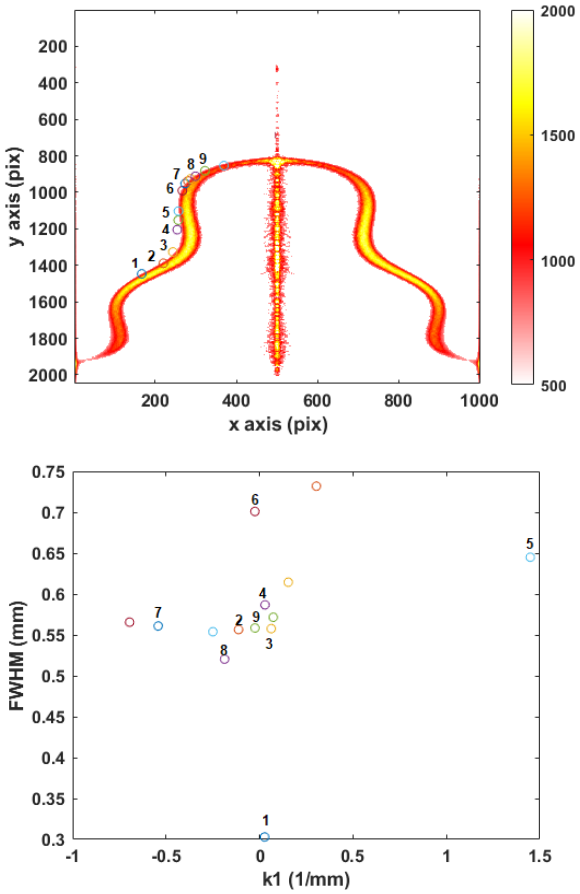

Fig. 5. Top) Inverted Abel transformed image of the flame response for φ=1.1 with the points of interest depicted in coloured loops and numbers. Bottom) Thickness vs k1 for the corresponding points.

Case studies for k_2 and maximum intensity have been provided in the supplementary document. Each of the equivalence ratio cases has been detailed and is provided below.

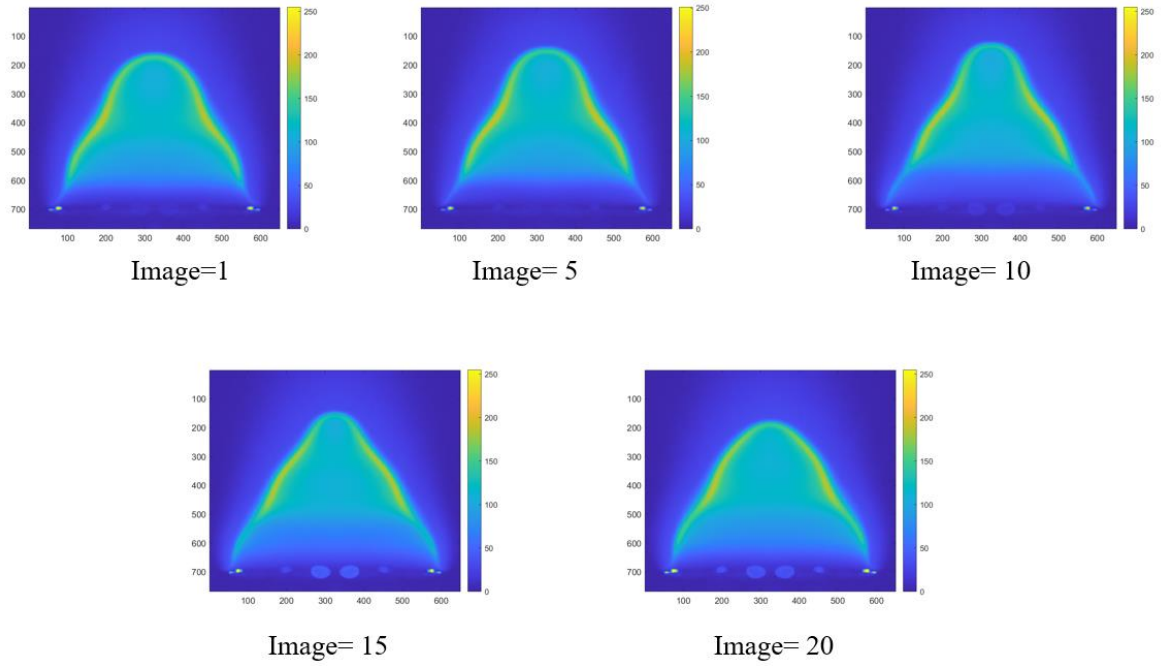

Fig. 6. Flame response at different instants at φ=1.1 for a forcing frequency of 40 Hz.

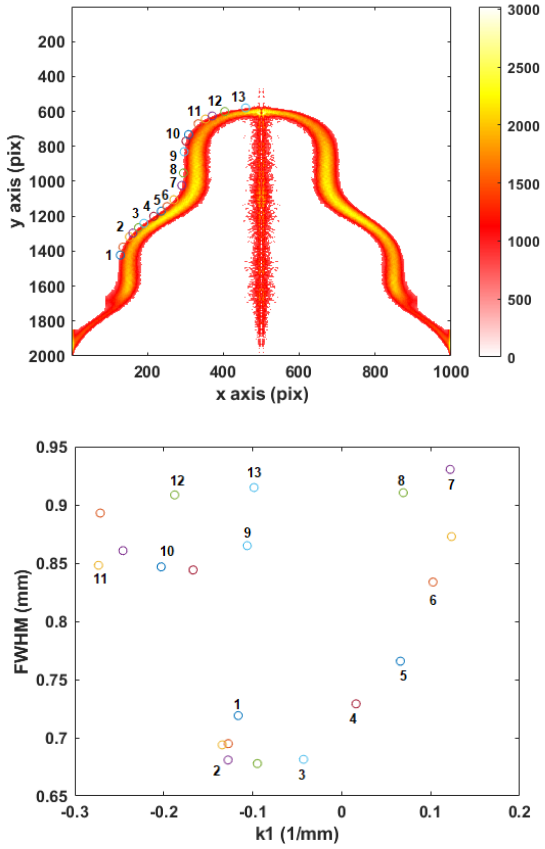

Fig. 7. Top) Inverted Abel transformed image of the flame response for φ=1.2 with the points of interest depicted in coloured loops and numbers. Bottom) Thickness vs k1 for the corresponding points.

For each case, a thickness vs k_1 graph along with an Inverse Abel transformed image of the desired flame mode captured at an instant is provided.

In each of the cases represented, understanding the thickness vs the curvature graph is a tedious process. The reader is advised to start with the coloured point on the base of the flame, identify the corresponding point with the help of the direction of the curvature in the thickness vs k_1 plot and move along the direction keeping in mind that each subsequent colour on the flame contour image is the colour to be looked out for in the thickness vs k_1 graph. A sequence of numbers has been provided to aid the reader in understanding the sense of the direction.

Case 1. φ=1.0

In the case of φ=1.0, Le=1 [18], which means that both thermal and molecular diffusion play an equally important role. It can be seen that the thickness does not vary a lot along the contour of the flame front. The effect of k_1 on the thickness is not very evident in this case. Since both thermal and diffusive effects play an equally important role, the thickness seems to be uniform all along the contour. Upon examining the evolution of the intensity along the contour, it can be seen that there is enhanced intensity towards the sides of the flame, similar to the case of the respective non-perturbed flame. To see the evolution of this intensity as a function of curvature, different modes must be captured. Figure 4 depicts this case study.

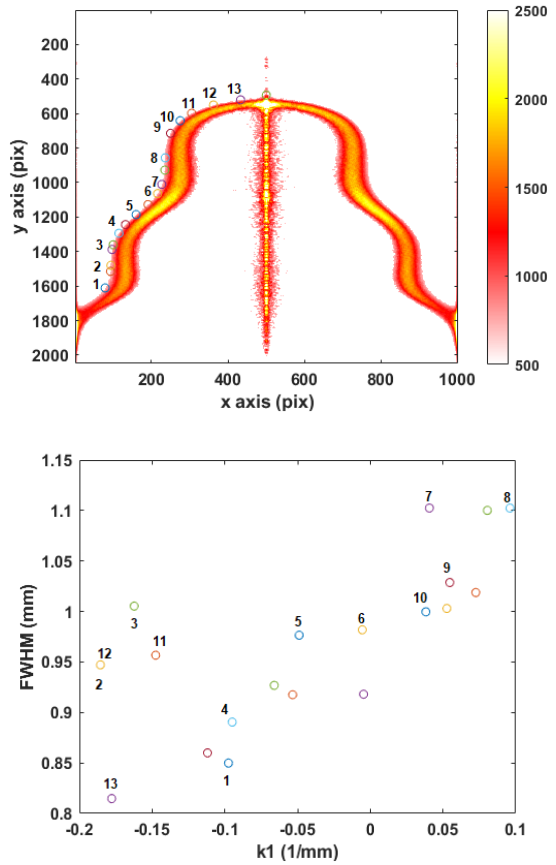

Fig. 8. Top) Inverted Abel transformed image of the flame response for φ=1.3 with the points of interest depicted in coloured loops and numbers. Bottom) Thickness vs k1 for the corresponding points.

Case 2. φ=1.1

At φ=1.1, Le=1.1 [18]. This implies that the thermal diffusion from the burnt gas towards the fresh gas happens at a slightly higher pace than the molecular diffusion of fresh gas into the burnt gas. Figure 5 depicts this case. A slight variation of the thickness along the contour can be seen. The front gets thinner when a negative k_1 is encountered and gets thicker when a positive k_1 is encountered. On examining the intensity, it can be seen that the reactivity is well-enhanced towards the sides of the flame. In Figure 5, it is seen that irrespective of a positive or a negative curvature, there is no change in the maximum intensity towards the sides of the flames. Since, the relatively higher magnitude of the curvature does not have a major impact on the reactivity of these flames, it is insinuated that rather than having a major curvature effect on the front, the preferential diffusion effects play a larger role. Figure 6 represents the different flame response modes captured for the same perturbation conditions at different instances. It can be seen that the relative intensity is enhanced at the sides of the flame irrespective of the curvature being positive or negative. It may be concluded that a large-scale preferential diffusion effect of H_2 plays a pivotal role.

Case 3. φ=1.2

In the case of, φ=1.2, Le increases slightly [18]. With an increase in the equivalence ratio, while almost maintaining the value of Le, this case shows a more prominent difference in the thickness vs curvature trends. The transition from a negative k_1 to a positive k_1 with thickness changing can be seen in Figure 7. In this case, it can be noted that the maximum intensity along the contour varies as a function of the orientation of the curvature. Here, for a negative curvature, along with a thinner front, the local maximum intensity is higher than for the case of a positive curvature where the front is thicker and the intensity is reduced. As mentioned by Chen et al. [22] for the case of non-perturbed flames φ=1.2, the enhancement of reactivity at the tip of the flame (negative curvature) is due to the enhanced production of H_2 which is strongly influenced by the curvature. Here, an inverse effect is seen for a positive curvature. However, it can be confirmed that the local preferential diffusion of H_2 promoted by the induced curvature and due to the Le effect is not the only parameter that controls the flame response.

From Figure 7, it can be seen that for the same values of k_1, the thickness values are not the same (Points 1, 9 and 13) and the magnitude of the maximum intensity for the same value of the curvature decreases when moving from the bottom to the top of the flame. These three points are located at three different positions along the contour. For the point further downstream, the value of the thickness was higher and the intensity was lower implying that it is not just k_1 that influences thickness but there is still a large-scale preferential diffusion that influences the reactivity which results in affecting the thickness and the magnitude of intensity. This is further discussed later in the case studies. However, the magnitude of this change in thickness and intensity is not large and so, it may be said that the local preferential diffusion plays a stronger role.

Case 4. φ=1.3

For φ=1.3 with Le=1.09 [18], the trend of the thickness vs k_1 is quite similar to φ=1.2. However, the variation of the thickness is much higher than that of φ=1.2 and the magnitude of k_1 is lower than φ=1.2. Similar to the previous case, a change of intensity and thickness as a function of the orientation of the curvature is noticed once again implying that the local preferential diffusion of H_2 plays an important role. Figure 8 represents this case.

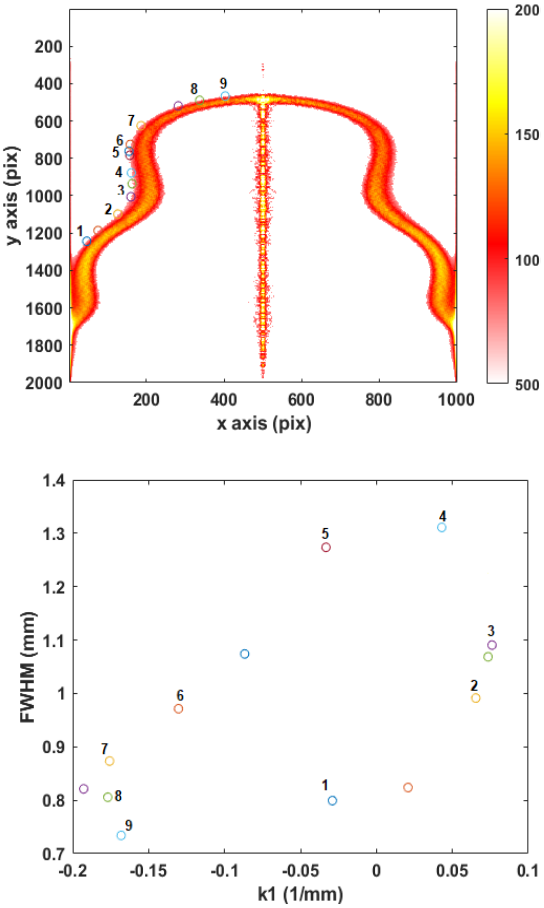

Fig. 9. Top) Inverted Abel transformed image of the flame response for φ=1.4 with the points of interest depicted in coloured loops and numbers. Bottom) Thickness vs k1 for the corresponding points.

Case 5. φ=1.4

For φ=1.4, the value of the Lewis number is slightly higher than 1. The range of the values of k_1 for φ=1.4 and φ=1.3 is the same but the variation in thickness for φ=1.4 is higher than φ=1.3 implying that change of thickness as a function of k_1 is more prominent for highly rich flames. Figure 9 represents this case. As demonstrated in Case 3, it can be seen again that for the same value of k_1 (Points 1 and 5), the thickness is not the same as these two points correspond to different locations along the flame. As seen for cases 3 and 4, a local preferential diffusion enhanced due to the curvature is seen. As the flames get thicker, it is important to note that the curvature calculated at the outer contour (as done here) may not be the same as the values that will be obtained when computing at the inner contour. For consistency, only the outer contours have been used for all the cases.

From all of these cases, it is quite apparent that irrespective of the condition, a negative k_1 results in the reduction of the thickness and a positive k_1 manifests as an increase in thickness. In the supplementary data, both k_1 vs contour of the flame and thickness vs contour of the flame for each of the cases have been provided. Globally, it was seen that the intensity decreases when moving away from the flame base owing to the large-scale preferential diffusion. For near stoichiometric conditions, it was a continuously decreasing trend whereas, for richer flames, the intensity decreased and increased as a function of the orientation of the curvature with a tendency towards decreased intensity when moving from the bottom to the top of the flame. This phenomenon was captured in the case of φ =1 and 1.1 but also for φ = 1.2 (Points 1, 9 and 13) and φ = 1.4 (Fig. 9, Points 1 and 5) where on plotting k_1 vs thickness where the thickness was different for the same value of k_1 at different positions along the contour. It was also seen that there is a local preferential diffusion of lighter species due to curvature for richer flames. The Damköhler number, Da, is defined as the ratio of the flow time scales to the chemical time scales. The chemical time scale can be obtained by dividing the thickness of the flame by the laminar flame speed. Da of these case studies was close to 1, implying that the time scale of the forced perturbation on the flow was comparable to the chemistry time scale. The effect of the perturbation on the flow is seen as a local change of thickness with respect to the orientation of k_1 along with the local Le of the flame determining a major role in the flame response. It may also be concluded that for the studied cases, the preferential diffusion effects play a large role in any changes of reactivity and as far as curvature effects are concerned, the effect of k_1 can be seen as a change of thickness for the near stoichiometric conditions.

Conclusions

One of the first experimental tests on flame-acoustic interactions for premixed ammonia air mixtures has been investigated with the objective of studying the effect of curvature on the reactivity of the flames. These experiments were performed on a Bunsen burner at atmospheric conditions for φ=0.9-1.4 for non-perturbed and φ=1.0-1.4 for perturbed flames with an acoustic perturbation of forcing frequency of 40 Hz. NH_2* was monitored as this species would give direct information on the heat release rate. On studying the non-perturbed cases, it was seen that lean and near stoichiometric flames displayed a local increase in intensity towards the sides of the flame which is attributed to the preferential diffusion of lighter species as the convective velocity of the flow was higher than the diffusion velocity of ammonia. It was understood that ammonia decomposes into H_2 which diffuse faster towards the sides of the flames. For richer flames, Le>1, with the increase in the production of H_2, the large-scale preferential

diffusion still exists but is not apparent as for the leaner cases. In the perturbed studies, it was seen that irrespective of the equivalence ratio, positive k_1 lead to an increase in the front thickness whereas a negative k_1 lead to a decrease in the front thickness. Once again, the preferential diffusion of H_2 played a major role. For near stoichiometric conditions, the quantity of H_2 produced is low and so a large-scale preferential diffusion towards the sides of the flame was witnessed despite the fact that these flames responded with higher magnitudes of curvature to the same acoustic perturbations. It was established from a preliminary analysis that weak flames are more affected by perturbations, however, it is the selective diffusion of H_2 that is more susceptible to change in curvatures leading to a local enhancement of reactivity. For richer flames, the local production of H_2 was promoted for negative curvatures which were seen as a local increase in intensity and decrease in thickness. Unlike the leaner perturbed cases, a local preferential diffusion effect superimposed with a large-scale preferential diffusion effect was witnessed. Since Da~1, the reaction and perturbation time scales are comparable. The effect of curvature was manifested as a change in the thickness of the contour for all cases. The effect of local preferential diffusion was seen as a function of orientation of the curvature for richer flames. Like the non-perturbed cases, a global decrease in intensity owing to the large-scale preferential diffusion is seen. Indeed, this case study alone is quite complex with multiple factors playing significant roles simultaneously. On analysing the non-perturbed cases, the role of preferential diffusion in ammonia flames is better understood. For the given experimental set-up, the flow conditions are of low speeds and so, conditions like Da<<1 which is ideal to isolate the effects of the acoustic perturbation on both lean and rich flames could not be explored. Nevertheless, from this study, it can be concluded that for richer flames where Le>1, there is an inhibition in the production of hydrogen at positive curvatures. To enhance reactivity (as a function of both intensity and thickness of the front) in these conditions, a negative curvature can help with the local production of hydrogen (increase in intensity and reduction in thickness).

Competing interests

The authors have no competing interest to declare.

References

1. Xiao H, Valera-Medina A, Bowen P and Dooley S, 3D Simulation of Ammonia Combustion in a Lean Premixed Swirl Burner, *Energy Procedia* 2017; 142: 1294. https://doi.org/10.1016/j.egypro.2017.12.504.

2. Hussein NA, Valera-Medina A and Alsaegh AS. Ammonia- hydrogen combustion in a swirl burner with reduction of NOx emissions, *Energy Procedia*. 2019; 158: 2305. https://doi.org/10.1016/j.egypro.2019.01.265

3. Lhuillier C, Brequigny P, Contino F and Mounaïm-Rousselle C. Experimental investigation on ammonia combustion behavior in a spark-ignition engine by means of laminar and turbulent expanding flames, *Proc. Combust. Inst.* 2021; 38: 5859. https://doi.org/10.1016/j.proci.2020.08.058

4. Fan Q, Liu X,Xu L, Subash AA, Brackmann C, Aldén M, Bai X-S and Li Z. Flame structure and burning velocity of ammonia/air turbulent premixed flames at high Karlovitz number conditions, *Combust. Flame.* 2022; 238: 111943. https://doi.org/10.1016/j.combustflame.2021.111943

5. Zitouni S, Brequigny P and Mounaïm-Rousselle C. Turbulent flame speed and morphology of pure ammonia flames and blends with methane or hydrogen, *Proc. Combust. Inst.* 2022; S1540748922002073. https://doi.org/10.1016/j.proci.2022.07.179

6. Mong GR, Chiong M-C, Chong CT, Ng J-H, Mashruk S, Tran M-V, Lee KM, Samiran NA, Wong KY, et al., Fuel-lean ammonia/biogas combustion characteristics under the reacting swirl flow conditions, *Fuel*. 2023; 331: 125983. https://doi.org/10.1016/j.fuel.2022.125983

7. Hashimoto G, Hadi K, Xia Y, Hamid A, Hashimoto N, Hayakawa A, Kobayashi H and Fujita O. Turbulent flame propagation limits of ammonia/methane/air premixed mixture in a constant volume vessel, *Proc. Combust. Inst.* 2021; 38: 5171. https://doi.org/10.1016/j.proci.2020.08.055

8. Khateeb AA, Guiberti TF, Wang G, Boyette WR, Younes M, Jamal A and Roberts WL. Stability limits and NO emissions of premixed swirl ammonia-air flames enriched with hydrogen or methane at elevated pressures, *Int. J. Hydrog. Energy*. 2021; 46: 11969. https://doi.org/10.1016/j.ijhydene.2021.01.036

9. Somarathne KDKA, Hatakeyama S, Hayakawa A and Kobayashi H. Numerical study of a low emission gas turbine like combustor for turbulent ammonia/air premixed swirl flames with a secondary air injection at high pressure, *Int. J. Hydrog. Energy*. 2017; 42: 27388. https://doi.org/10.1016/j.ijhydene.2017.09.089

10. Netzer C, Ahmed A, Gruber A and Løvås T. Curvature effects on NO formation in wrinkled laminar ammonia/hydrogen/nitrogen-air premixed flames. *Combust. Flame.* 2021; 232: 111520. https://doi.org/10.1016/j.combustflame.2021.111520

11. Wei X, Zhang M, An Z, Wang J, Huang Z and Tan H. Large eddy simulation on flame topologies and the blow-off characteristics of ammonia/air flame in a model gas turbine combustor, *Fuel*. 2021; 298: 120846. https://doi.org/10.1016/j.fuel.2021.120846
12. Wan Z, Tao Y, Shao J, Zhang Y and You H. Ammonia as an effective hydrogen carrier and a clean fuel for solid oxide fuel cells, *Energy Convers. Manag.* 2021; 228: 113729. https://doi.org/10.1016/j.enconman.2020.113729
13. Sun S, Jiang Q, Zhao D, Cao T, Sha H, Zhang C, Song H and Da Z. Ammonia as hydrogen carrier: Advances in ammonia decomposition catalysts for promising hydrogen production, *Renew. Sustain. Energy Rev.* 2022; 169: 112918. https://doi.org/10.1016/j.rser.2022.112918
14. Juangsa FB, Irhamna AR and Aziz M. Production of ammonia as potential hydrogen carrier: Review on thermochemical and electrochemical processes, *Int. J. Hydrog. Energy*. 2021; 46: 14455. https://doi.org/10.1016/j.ijhydene.2021.01.214
15. Rieth M, Gruber A, Williams FA and Chen JH. Enhanced burning rates in hydrogen-enriched turbulent premixed flames by diffusion of molecular and atomic hydrogen, *Combust. Flame*. 2022; 239: 111740. https://doi.org/10.1016/j.combustflame.2021.111740
16. Karan A, Dayma G, Chauveau C and Halter F. Insight into the inner structure of stretched premixed ammonia-air flames, *Proc. Combust. Inst.* 2022: S1540748922001067. https://doi.org/10.1016/j.proci.2022.07.066
17. Birbaud AL, Durox D and Candel S. Upstream flow dynamics of a laminar premixed conical flame submitted to acoustic modulations, *Combust. Flame*. 2006; 146: 541. https://doi.org/10.1016/j.combustflame.2006.05.001
18. Ichimura R, Hadi K, Hashimoto N, Hayakawa A, Kobayashi H and Fujita O. Extinction limits of an ammonia/air flame propagating in a turbulent field, *Fuel*. 2019; 246: 178. https://doi.org/10.1016/j.fuel.2019.02.110
19. Dandy D. *Bioanalytical Microfluidics Program. Color State Univ*. https://navier.engr.colostate.edu/
20. Mizomoto M, Asaka Y, Ikai S and Law CK. Effects of preferential diffusion on the burning intensity of curved flames, *Symp. Int. Combust.* 1985; 20: 1933. https://doi.org/10.1016/S0082-0784(85)80692-5
21. Stagni A, Cavallotti C, Arunthanayothin S, Song Y, Herbinet O, Battin-Leclerc F and Faravelli T. An experimental, theoretical and kinetic-modeling study of the gas-phase oxidation of ammonia, *React. Chem. Eng.* 2020; 5: 696. https://doi.org/10.1039/C9RE00429G
22. Chen J, Fan W and Zhang H. Experimental and numerical study of curvature effects and NO formation in ammonia Bunsen flames, *Fuel*. 2023; 345: 128207. https://doi.org/10.1016/j.fuel.2023.128207
23. Matalon M and Matkowsky BJ. Flames as gasdynamic discontinuities, *J. Fluid Mech.* 1982; 124: 239. https://doi.org/10.1017/S0022112082002481
24. Candel SM and Poinsot TJ. Flame Stretch and the Balance Equation for the Flame Area, *Combust. Sci. Technol.* 1990; 70: 1. https://doi.org/10.1080/00102209008951608
25. Clavin P and Joulin G. Premixed flames in large scale and high intensity turbulent flow, *J. Phys. Lett.* 1983; 44: 1. https://doi.org/10.1051/jphyslet:019830044010100
26. Thiesset F, Halter F, Bariki C, Lapeyre C, Chauveau C, Gökalp I, Selle L and Poinsot T. Isolating strain and curvature effects in premixed flame/vortex interactions, *J. Fluid Mech.* 2017; 831: 618. https://doi.org/10.1017/jfm.2017.641